Journal of Applied Electrochemistry **34**: 501–506, 2004.

Electrochemical removal of tin from dilute aqueous sulfate solutions using a rotating cylinder electrode of expanded metal

J.C. BAZAN and J.M. BISANG*
Programa de Electroquímica Aplicada e Ingeniería Electroquímica (PRELINE), Facultad de Ingeniería Química (UNL), Santiago del Estero 2829, S3000AOM Santa Fe, Argentina
*(*author for correspondence, fax: +54 342 4571162, e-mail: jbisang@fiqus.unl.edu.ar)*

Received 15 July 2003; accepted in revised form 19 November 2003

Key words: electrochemical effluent treatment, expanded metal, rotating cylinder electrode, tin removal

Abstract

The performance of a batch undivided electrochemical reactor with a rotating cylinder electrode of expanded metal sheets for the removal of tin from synthetic sulfate solution is studied. The effect of the cathode potential, initial tin concentration, number of sheets forming the cathode and cathodic side reactions on the figures of merit of the reactor is analysed. For a cathode potential of −0.65 V vs SCE at 500 rpm, the tin concentration decreased from 393 to 94 mg l^{-1} after 30 min of electrolysis with a specific energy consumption of 3.93 kWh kg^{-1} and a normalized space velocity of 1.27 h^{-1}. The change in concentration was higher when the potential was more negative because of the turbulence-promoting action of the hydrogen evolution. The results suggest that the applied potential must represent a compromise between the increase in space time yield or normalized space velocity and the increase in the specific energy consumption.

List of symbols

a_e	reactor specific surface area (m^{-1})
A_s	electrode specific surface area (m^{-1})
C	concentration (mg l^{-1} or kg m^{-3})
d_h	hydraulic diameter $= 6\varepsilon/A_s$ (m)
D	diffusion coefficient (m^2 s^{-1})
E_{SCE}	cathode potential referred to saturated calomel electrode (V)
E_s	specific energy consumption (W s kg^{-1} or kWh kg^{-1})
F	faradaic constant (C mol^{-1})
h	interelectrode gap (m)
i	current density (A m^{-2})
i_{lim}	limiting current density (A m^{-2})
I	total current (A)
k	mass-transfer coefficient (m s^{-1})
l	bed thickness parallel to the current flow (m)
M	atomic weight (g mol^{-1})
Q	volumetric flow rate (m^3 s^{-1})
r_1	internal radius (m)
r_2	external radius (m)
$\bar{r}$	mean radius $= \sqrt{(r_1^2 + r_2^2)/2}$ (m)
Re_c	channel Reynolds number $= Q/h\varepsilon v$
Re_r	rotating Reynolds number $= \omega r_2^2/v$
Sc	Schmidt number $= v/D$
Sh	Sherwood number $= kd_h/D$
s_n	normalized space velocity (s^{-1} or h^{-1})
t	time (min or s)
U	cell voltage (V)
V	effective electrolyte volume within the reactor (m^3)
x	fractional conversion

Greek symbols

β	current efficiency (%)
$\Delta\eta$	admitted range of overpotential (V)
ε	porosity
v	kinematic viscosity (m^2 s^{-1})
v_e	charge transfer of the electrode reaction
ρ_{mean}	space time yield (kg m^{-3} s^{-1})
ρ_s	effective electrolyte resistivity (Ω m)
ω	rotation speed (s^{-1})

1. Introduction

Tin is a valuable metal and has been readily applied to all common metals, including aluminium, to impart corrosion and tarnish resistance, enhance surface appearance or improve solderability and electrical conductivity. A potentially useful source of tin is the waste streams from processes such as (a) tin electroplating, (b) aluminium anodizing, (c) the manufacture of printed circuits boards and (d) metal-pickling processes or the detinning of scrap. Thus, the development of technologies to recover tin from effluents is justified and the processing of such solutions is attractive environmentally.

There are many possible methods of tin recovery including solvent extraction [1], ion exchange [2], and electrolysis. However, very little work has been done on the electrolytic recovery of tin from dilute solutions. The electrochemical processing of effluents requires the use of equipment with a high value of the product of the mass-transfer coefficient and the active electrode area, in order to increase the space time yield. Thus, Chaudhary et al. [3] reported the removal of tin from chloride solutions using an electrochemical reactor with mesh electrodes immersed in a fluidized bed of inert glass beads. Another strategy to achieve a combination of good mass-transfer conditions with high conversion per pass is the use of the rotating cylinder electrode [4]. Additionally, Kreysa and Brandner [5] and Nahlé et al. [6] reported that the performance of rotating electrodes can be enhanced by using a three dimensional structure.

The purpose of this work is the analysis of the behaviour of an undivided electrochemical reactor with a rotating packed bed electrode of expanded metal sheets for the removal of tin and the study of the process variables, such as initial tin concentration, cathode potential, bed thickness and the influence of the side cathodic reactions on the 'figures of merit' of the reactor.

2. Fundamental studies with a rotating disc electrode

The working electrode was a tin rotating disc (dia. 5 mm) embedded in a Teflon bell of 34.5 mm base diameter. The counterelectrode was a platinum wire (dia. 0.7 mm and 0.105 m long) and as reference a saturated calomel electrode was used. The potentials are referred to this electrode. All experiments were performed at 30 °C under a slow potentiodynamic sweep of 1 mV s^{-1}. The solution was approximately 4×10^{-3} M tin (475 mg l^{-1}), prepared from reagent grade tin(II) sulfate, with 1 M Na_2SO_4 as supporting electrolyte at pH 4. Prior to each experiment the exact tin(II) concentration was complexometric determined by direct titration with standard 0.1 M EDTA [7] as the titrant and the tin(IV) concentration by indirect complexometric titration with lead(II) [8] with an accuracy of ±1%. It was observed that tin(II) was rapidly oxidized by the dissolved oxygen and tin(II) was only detected in small concentrations in recently prepared solutions. Thus, tin(IV) was always the predominant species. Tin(IV) is easily hydrolysed [9] and the formation of a sludge of basic tin compounds takes place, which produces turbidity in the solution.

Figure 1 shows typical polarization curves at different angular velocities. It can be seen that tin deposition begins at −0.525 V and a limiting current is reached at about −0.6 V. The current density shows a plateau over a narrow range of potentials, lower than 0.1 V, because of the onset of hydrogen evolution. Thus, taking into account the potential distribution in three-dimensional electrodes, the electrode thickness parallel to the current flow must be restricted. A plot of $1/i$ against $1/\omega^{1/2}$ is included as an inset in Figure 1 for a potential of −0.625 V. From the slope of the line the tin(IV) diffusion coefficient (D) is $1.0 \pm 0.1 \times 10^{-10}$ m^2 s^{-1}. This low value of D may be attributed to the formation of complex ions in the electrolyte.

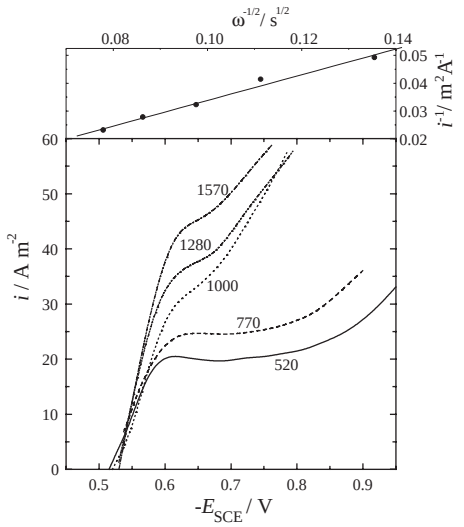

Fig. 1. Current density as a function of the electrode potential for tin rotating disc electrodes at different angular velocities in rpm. Scan rate 1 mV s^{-1}. $T = 30$ °C. Electrolyte 1 M Na_2SO_4, $C \cong 475$ mg l^{-1}, pH ≅ 4. Inset: $1/i$ against $1/\omega^{1/2}$ for a potential of −0.625 V.

3. Tin removal with a rotating three-dimensional electrode

3.1. *Experimental details*

The experiments were performed in an undivided batch reactor (95 mm int. dia. and 140 mm high). The reactor was thermostatted by a heating jacket. The working electrode was a rotating cylinder made by ordered packing of expanded metal sheets of 316 stainless steel (35 mm int. dia. and 33 mm long). Table 1 gives the geometrical characteristics of the expanded metal. The lower part of the electrode was open but the upper part was joined to a Teflon sleeve in order to orientate the electrolyte flow through the sheet pack. A perforated disc, centrally positioned and rendered inactive with an

Table 1. Geometrical characteristics of the expanded metal

Characteristic parameter	
Long diagonal/mm	10
Short diagonal/mm	5
Long mesh aperture/mm	8
Short mesh aperture/mm	4
Thickness/mm	0.36
Apparent thickness/mm	1.2
Strand width/mm	0.7
Surface area per unit volume of electrode/m^{-1}	766 ± 22
Surface area per unit net area	0.92 ± 0.03

epoxy coating, was used as current feeder and also as support of the three-dimensional electrode.

The expanded sheets were arranged with the large diagonal parallel to the rotation axis. Thus, there were two possibilities for the orientation of the mesh with respect to the electrode rotation sense, which were previously reported in [10]. In variant 1 the strands of the expanded structure form an acute angle with the plane of the metal sheet, thus the expanded material deflects the electrolyte towards the outer region of the electrode, while in variant 2 the deflection is towards the inner region of the electrode. Variant 1 only was used in this study because it offers the best performance for the reactor [10]. The three-dimensional electrode was arranged with a perfect superposition of the metal expanded sheets, which defines straight interconnected pores perpendicular to the rotation axis and diminishes the apparent thickness to 0.95 mm. The cathode thickness for four sheets was 3.8 mm, which is the optimum bed depth according to the following analytical expression [11]:

$$l = \left(\frac{2\Delta\eta}{\rho_s A_s i_{lim}}\right)^{0.5} \tag{1}$$

For the calculation of the optimum bed depth it was assumed that $\Delta\eta = 0.1$ V, $\rho_s = 0.12\ \Omega$ m, $A_s = 766\ \text{m}^{-1}$ and $i_{lim} = 89.85\ \text{A m}^{-2}$. The limiting current density was calculated for 500 mg l^{-1} tin(IV) concentration with a mass-transfer coefficient according to a previous correlation [12], neglecting the convective Reynolds number of the channel. Thus, the whole bed is working under limiting current conditions.

As counterelectrode three platinum wires (dia. 1 mm and 90 mm long) placed symmetrically were used. The working electrode and the counterelectrode were concentric, thereby assuring a uniform primary current distribution. The interelectrode gap was 11 mm. As reference a saturated calomel electrode was used and the potentials are referred to this electrode. Prior to each experiment the working electrode was washed with hydrochloric acid in an ultrasonic cleaner. All experiments were performed at 30 °C under potentiostatic control. The electrode reactions were oxygen evolution at the anode and tin deposition, from the oxidation state +4, at the cathode. Hydrogen evolution and oxygen reduction took place as cathodic side reactions.

The supporting electrolyte was 1 M Na_2SO_4 with an initial tin concentration in the range 150–500 mg l^{-1} at about pH 4. Samples of solution were taken from the reactor and the tin concentration was measured by atomic absorption spectroscopy, in order to determine the variation of concentration with time and the differential concentration decrease. From these data the current efficiency, the space time yield, the normalized space velocity and the specific energy consumption were calculated. The solution volume in each experiment was 0.6 l.

3.2. *Mathematical model*

For a rotating cylinder electrode the electrolyte is assumed to be well-mixed at all times. Thus, for a batch reactor in the potential range where the tin deposition is mass-transfer controlled, the change of concentration with time is given by

$$C(t) = C(0)\exp(-ka_e t) \tag{2}$$

Therefore, the mass-transfer coefficient has to be evaluated in order to discuss the results obtained experimentally. Using as test reactions the reduction of ferricyanide on nickel plated steel spheres or the silver deposition on graphite particles, Kreysa [12] proposed the following expression to calculate the mass-transfer coefficient for a rotating packed bed electrochemical reactor:

$$Sh = 0.454\, Sc^{1/3}\left[Re_c^2 + \left(Re_r \frac{d_h}{\varepsilon \bar{r}}\right)^2\right]^{0.290}\left(\frac{d_h}{r_2 - r_1}\right)^{1.116} \tag{3}$$

In the present study there is no contribution of the channel Reynolds number on the mass-transfer coefficient.

The fractional conversion and the accumulative current efficiency as a function of time are given by

$$x(t) = 1 - \exp(-ka_e t) \tag{4}$$

and

$$\beta(t) = \frac{v_e FVC(0)x(t)}{M\int_0^t I(t)\mathrm{d}t} \tag{5}$$

Other 'figures of merit' used to compare the performance of the electrochemical reactor are the mean value of the space time yield, the normalized space velocity and the specific energy consumption, which were calculated with the following equations:

$$\rho_{mean}(t) = \frac{C(0)x(t)}{t} \tag{6}$$

$$s_n(t) = -\frac{\ln[1 - x(t)]}{t \ln 10} \tag{7}$$

and

$$E_s(t) = \frac{\int_0^t U(t)I(t)\mathrm{d}t}{VC(0)x(t)} \tag{8}$$

3.3. *Results and discussion*

Figure 2 shows the current as a function of time for different values of the bed thickness at −0.65 V. The

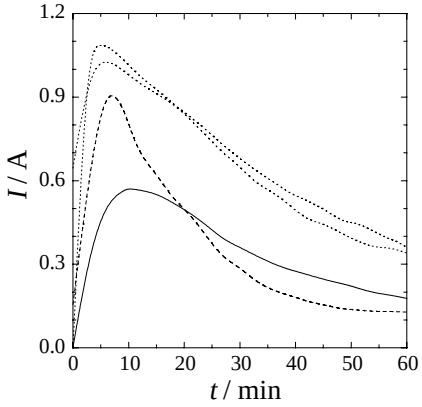

Fig. 2. Current as a function of time for different number of sheets of expanded metal. Full line: 1 nets, dashed line: 2 nets and dotted lines: two experiments with 4 nets. $E_{SCE} = -0.65$ V. $\omega = 500$ rpm. $T = 30$ °C. Electrolyte 1 M Na_2SO_4, $C(0) \cong 400$ mg l^{-1}.

dotted lines correspond to two experiments with four sheets of expanded metal. The differences between them can be attributed to the roughness of the electrode produced by the tin deposition; nevertheless, the reproducibility of the experiments is acceptable. Likewise, the curves of Figure 2 show a maximum, which is the consequence of two opposite effects. On one hand the tin deposition increases, due to the increase in the roughness, the electrode area and thus the total current. On the other hand, in a batch reactor the tin concentration decreases with time. The second factor predominates over the first at high times and the current shows a maximum. Likewise, at high times the tin concentration diminishes and the measured current can be attributed to the presence of side cathodic reactions. This current against time behaviour in Figure 2 is similar to that reported by Gabe and Walsh [13] for copper deposition at a rotating cylinder electrode.

Figure 3 shows the tin concentration as a function of time for different values of the initial tin concentration, number of expanded metal sheets and cathodic potential. There is a pronounced decrease in concentration during the first stages of the experiments, but at high times the concentration approaches a constant value. Part (b) of Figure 3 shows that the concentration change increases when the number of sheets increases but the experimental results for two and four sheets are very similar. Part (c) of Figure 3 reports the effect of potential on the concentration change. At short times, the concentration change increases when the potential becomes more negative. This behaviour can be explained by the fact that at these potentials the mass-transfer coefficient is enhanced by the turbulence-promoting action of hydrogen evolution, which takes place as the side cathodic reaction.

In Figure 4 the experimental results of Figure 3 are replotted according to the dimensionless logarithmic form of Equation 2. The full line represents the theoretical behaviour with a mass-transfer coefficient calculated from Equation 3. Within the accuracy nor-

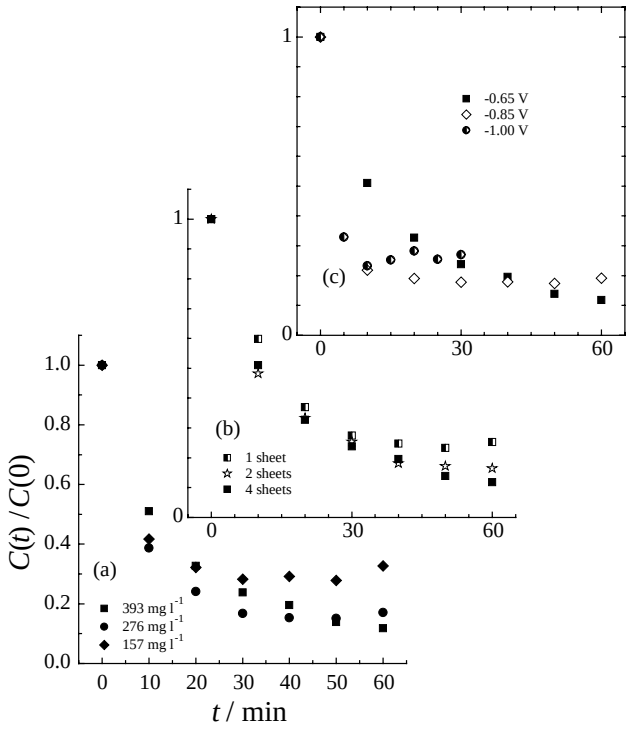

Fig. 3. Normalized tin concentration as a function of time. Part (a): $E_{SCE} = -0.65$ V, 4 sheets of expanded metal. Part (b): $E_{SCE} = -0.65$ V, $C(0) \cong 400$ mg l^{-1}. Part (c): $C(0) \cong 350$–400 mg l^{-1}, 4 sheets of expanded metal. $\omega = 500$ rpm. $T = 30$ °C. Supporting electrolyte 1 M Na_2SO_4.

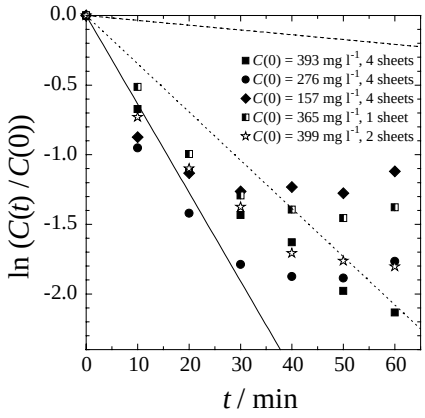

Fig. 4. Semi-logarithmic plot of normalized concentration as a function of time. $E_{SCE} = -0.65$ V. Full line: theoretical prediction according to Equations 2 and 3. Dashed line: Equation 2 with a mass-transfer coefficient according to Eisenberg et al. correlation [15]. Dotted line: Equation 2 with a mass-transfer coefficient according to Holland expression [16]. $\omega = 500$ rpm. $T = 30$ °C. Supporting electrolyte 1 M Na_2SO_4.

mally expected for this type of measurement, the experimental results obtained at a potential of −0.65 V are in close agreement with the theoretical prediction during the first stages of the experiment, in the range 0–20 min. For longer times, the slopes of the curves progressively decrease and the residual tin concentration is higher than the theoretical prediction. This behaviour was also observed by Robinson and Walsh [14] for

copper deposition and was attributed to a progressive change in the rate-determining process and to the redissolution of the metal by the oxygen generated at the anode. An additional contributory factor in the present study may be the redissolution of the sludge of basic tin compounds always present in the electrolyte. Figure 4 also shows the behaviour for a rotating cylinder electrode in a batch reactor with a mass-transfer coefficient calculated according to the correlations of Eisenberg et al. [15], valid for smooth electrodes and represented by the dashed line, and Holland [16], valid for metal powder deposition and represented by the dotted line. The higher decays in concentration showed by the expanded metal electrode can be attributed to the higher value of the specific surface area.

Figure 5 shows typical curves of the accumulative current efficiency as a function of time. For a potential of −0.65 V the current efficiency is close to 100% early in the experiment and decreases at higher times because the tin concentration decreases and the oxygen reduction predominates. For potentials more negative than −0.65 V hydrogen evolution possibly occurs as cathodic side reaction and lower values of current efficiencies are measured. Likewise, the effect of the number of sheets of expanded metal on the accumulative current efficiency is reported in Figure 6, where similar behaviour for all electrodes is observed.

Figure 7 shows the mean value of the space time yield and the normalized space velocity as a function of the cathode potential when the charge passed in the reactor is about 1.3 times the stoichiometric value. Because of the turbulence-promoting action of the hydrogen evolution a pronounced increase in ρ_{mean} and s_{n} occurs when the potential becomes more negative. Thus, for a given removal requirement, the size of the reactor is reduced.

The specific energy consumption as a function of the electrolysis time at a potential of −0.65 V for different values of the initial tin(IV) concentration is shown in Figure 8. As expected E_{s} increases with decreasing tin

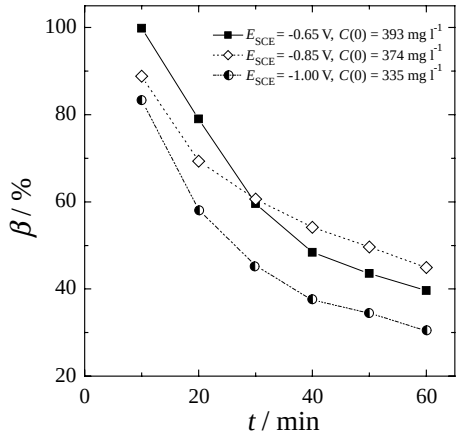

Fig. 5. Current efficiency as a function of time for different cathodic applied potentials. 4 sheets of expanded metal. $\omega = 500$ rpm. $T = 30$ °C. Supporting electrolyte 1 M Na_2SO_4.

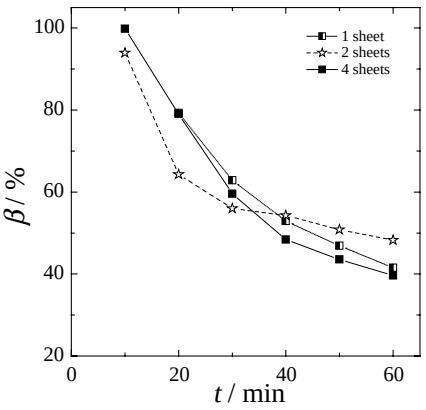

Fig. 6. Current efficiency as a function of time for different number of sheets of expanded metal. $E_{\text{SCE}} = -0.65$ V. $\omega = 500$ rpm. $T = 30$ °C. Supporting electrolyte 1 M Na_2SO_4. $C(0) \cong 400$ mg l^{-1}.

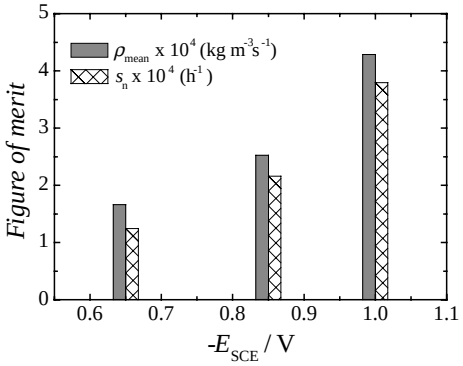

Fig. 7. Mean value of the space time yield and normalized space velocity as a function of the cathodic applied potential. 4 sheets of expanded metal. Ratio between the passed charge and the stoichiometric value ≅1.3. $\omega = 500$ rpm. $T = 30$ °C. Supporting electrolyte 1 M Na_2SO_4. $C(0) \cong 350$–400 mg l^{-1}.

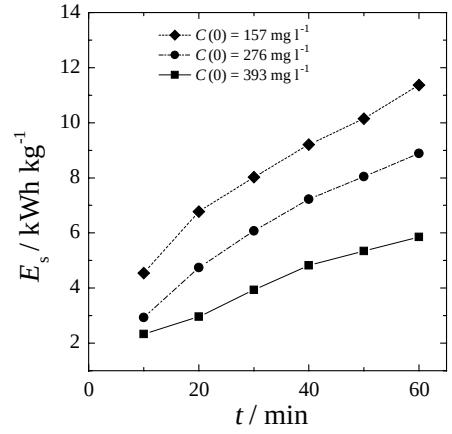

Fig. 8. Specific energy consumption as a function of time for different values of the initial tin concentration. 4 sheets of expanded metal. $E_{\text{SCE}} = -0.65$ V. $\omega = 500$ rpm. $T = 30$ °C. Supporting electrolyte 1 M Na_2SO_4.

concentration because the current efficiency decreases. Likewise, Figure 9 shows the specific energy consumption as a function of time for different applied potentials. The increase of E_{s} when the potential becomes

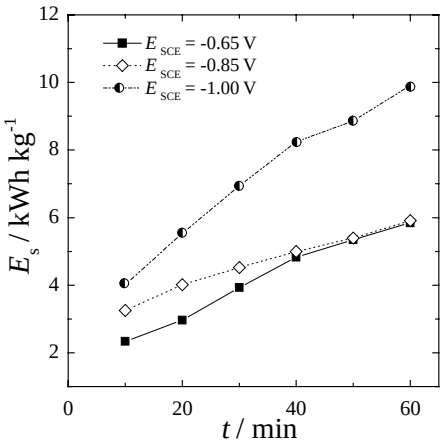

Fig. 9. Specific energy consumption as a function of time for different values of the cathodic applied potential. 4 sheets of expanded metal. $\omega = 500$ rpm. $T = 30$ °C. Supporting electrolyte 1 M Na_2SO_4. $C(0) \cong 350$–400 mg l^{-1}.

more negative can be attributed to a decrease in the current efficiency because of the onset of the hydrogen evolution. The specific energy consumptions are in accordance with the values reported by Chaudhary et al. [3]. Comparing Figures 7 and 9 it can be concluded that hydrogen evolution as side cathodic reaction presents both beneficial and detrimental aspects. Thus, when the applied potential becomes more negative both space time yield and specific energy consumption also increase and the choice of potential depends on a compromise between the initial investment cost and the energy cost.

4. Conclusions

The following conclusions may be drawn:

(i) It was demonstrated that tin removal from dilute aqueous solution can be performed efficiently in an electrochemical reactor with a three-dimensional rotating cylinder electrode of expanded metal sheets. The bed thickness parallel to the cathode current flow must be small due to the fact that tin deposition takes place at limiting current in a narrow range of potentials.

(ii) The tin concentration follows the expected theoretical behaviour during the first stages of the experiment.

(iii) Hydrogen evolution, as side cathodic reaction, is beneficial for tin removal because the turbulence promoting action increases the current for the main reaction and enhances the space time yield or the normalized space velocity. But at the same time it is detrimental to the specific energy consumption because the current efficiency decreases. The potential applied to the cathode represents a compromise between these factors.

Acknowledgements

This work was supported by the Agencia Nacional de Promoción Científica y Tecnológica (ANPCyT), Consejo Nacional de Investigaciones Científicas y Técnicas (CONICET) and Universidad Nacional del Litoral (UNL) of Argentina. The authors are grateful to Fine Chemical Laboratory of INTEC (CONICET-UNL) for performing the atomic absorption analysis.

References

1. K. Inoue, R.S. Mirvaliev, K. Yoshizuka, K. Ohto and S. Babasaki, *Solvent Extr. Res. Dev., Jpn.* **8** (2001) 21.
2. D.C. Szlag and N.J. Wolf, *Clean Prod. Process.* **1** (1999) 117.
3. A.J. Chaudhary, S.O.V. Dando and S.M. Grimes, *J. Chem. Technol. Biotechnol.* **76** (2001) 47.
4. F.C. Walsh, *in* D. Genders and N. Weinberg (Eds), 'Electrochemistry for a Cleaner Environment' (The Electrosynthesis Company, New York, 1992), pp. 101–159.
5. G. Kreysa and R. Brandner, *in* 'Modern Concepts in Electrochemical Reactor Design', Extended Abstracts of the 31st ISE Meeting, Venice, Italy, **2** (1980) H8.
6. A.H. Nahlé, G.W. Reade and F.C. Walsh, *J. Appl. Electrochem.* **25** (1995) 450.
7. E. Merck (Ed.), 'Métodos complexométricos de valoración con titriplex' (Complexometric methods of titration with titriplex), 3rd edn., (A.G. Merck, Darmstadt), p. 34 (in Spanish).
8. C.N. Reilley and A.J. Barnard Jr, *in* L. Meites (Ed.), 'Handbook of Analytical Chemistry' (McGraw-Hill, New York, 1963), pp. 3–188.
9. E.W. Abel, *in* J.C. Bailar Jr, H.J. Emeléus, R. Nyholm and A.F. Trotman-Dickenson (Eds), 'Comprehensive Inorganic Chemistry' Vol. 2 (Pergamon, Oxford, 1973), pp. 43–104.
10. J.M. Grau and J.M. Bisang, *J. Chem. Technol. Biotechnol.* **78** (2003) 1032.
11. G. Kreysa, *DECHEMA Monographs* **94** (1983) 123 (in German).
12. G. Kreysa, *Chem.-Ing.-Tech.* **55** (1983) 23 (in German).
13. D.R. Gabe and F.C. Walsh, *J. Appl. Electrochem.* **14** (1984) 565.
14. D. Robinson and F.C. Walsh, *Hydrometallurgy* **26** (1991) 115.
15. M. Eisenberg, C.W. Tobias and C.R. Wilke, *J. Electrochem. Soc.* **101** (1954) 306.
16. F.S. Holland, *Chem. and Ind.* (*London*). July (1978) 453.